HHS Public Access

Author manuscript

Neuroimage. Author manuscript; available in PMC 2015 October 15.

Published in final edited form as:

Neuroimage. 2014 October 15; 100: 544–557. doi:10.1016/j.neuroimage.2014.05.032.

Flexible modulation of network connectivity related to cognition in Alzheimer's disease

Donald G. McLaren[a,b,c,d], **Reisa A. Sperling**[a,b,d,e], and **Alireza Atria**[a,b,c,d]

Donald G. McLaren: dmclaren2@partners.org; Reisa A. Sperling: rsperling@rics.bwh.harvard.edu; Alireza Atria: atri@nmr.mgh.harvard.edu

[a]Department of Neurology, Massachusetts General Hospital, 15 Parkman Street, WACC 715, Boston, Massachusetts 02114, USA

[b]Athinoula A. Martinos Center for Biomedical Imaging, Department of Radiology, Massachusetts General Hospital, 149 Thirteenth Street, Charlestown, Massachusetts 02129, USA

[c]Geriatric Research, Education and Clinical Center, ENRM VA Medical Center, 200 Springs Road, Bedford, MA 01730, USA

[d]Harvard Medical School, 25 Shattuck Street, Boston, MA 02115, USA

[e]Center for Alzheimer Research and Treatment, Department of Neurology, Brigham and Women's Hospital, 221 Longwood Avenue, Boston, MA 02115, USA

Abstract

Functional neuroimaging tools, such as fMRI methods, may elucidate the neural correlates of clinical, behavioral, and cognitive performance. Most functional imaging studies focus on regional task-related activity or resting state connectivity rather than how changes in functional connectivity across conditions and tasks are related to cognitive and behavioral performance. To investigate the promise of characterizing context-dependent connectivity-behavior relationships, this study applies the method of generalized psychophysiological interactions (gPPI) to assess the patterns of associative-memory-related fMRI hippocampal functional connectivity in Alzheimer's disease (AD) associated with performance on memory and other cognitively demanding neuropsychological tests and clinical measures. Twenty-four subjects with mild AD dementia (ages 54–82, nine females) participated in a face-name paired-associate encoding memory study. Generalized PPI analysis was used to estimate the connectivity between the hippocampus and the whole brain during encoding. The difference in hippocampal-whole brain connectivity between encoding novel and repeated face-name pairs was used in multiple-regression analyses as an independent predictor for 10 behavioral, neuropsychological and clinical tests. The analysis revealed connectivity-behavior relationships that were distributed, dynamically overlapping, and task-specific within and across intrinsic networks; hippocampal-whole brain connectivity-behavior relationships were not isolated to single networks, but spanned multiple brain networks.

Corresponding author: Donald G. McLaren, Ph.D., Department of Neurology, 15 Parkman Street, Boston, MA 02114, Tel: 617.726.6214, Fax: 617.726.5760, dmclaren2@partners.org.

Importantly, these spatially distributed performance patterns were unique for each measure. In general, out-of-network behavioral associations with encoding novel greater than repeated face-name pairs hippocampal-connectivity were observed in the default-mode network, while correlations with encoding repeated greater than novel face-name pairs hippocampal-connectivity were observed in the executive control network ($p<0.05$, cluster corrected). Psychophysiological interactions revealed significantly more extensive and robust associations between paired-associate encoding task-dependent hippocampal-whole brain connectivity and performance on memory and behavioral/clinical measures than previously revealed by standard activity-behavior analysis. Compared to resting state and task-activation methods, gPPI analyses may be more sensitive to reveal additional complementary information regarding subtle within- and between-network relations. The patterns of robust correlations between hippocampal-whole brain connectivity and behavioral measures identified here suggest that there are 'coordinated states' in the brain; that the dynamic range of these states is related to behavior and cognition; and that these states can be observed and quantified, even in individuals with mild AD.

Keywords

functional MRI; functional connectivity; gPPI; episodic memory; biomarker; dementia

1. Introduction

The use of fMRI methods to reveal relationships between behavior and cognitive function, whether in cognitively normal individuals or in patients with cognitive impairments due to conditions such as Alzheimer's disease (AD), can be divided into three key areas: resting connectivity (Balthazar et al., 2014; Biswal et al., 1995; Damoiseaux et al., 2012; Fox et al., 2006; Kelly et al., 2008; Li et al., 2013; Sala-Llonch et al., 2012; Shehzad et al., 2014), evoked task-related activity (Atri et al., 2011; DeYoe et al., 1994; Diamond et al., 2007; Dolcos et al., 2013; Ewbank et al., 2009; Friston et al., 1995a; Friston et al., 1995b; McLaren et al., 2012b; Putcha et al., 2011; Simon et al., 2010; Wig et al., 2008), and more recently context-dependent connectivity (Chatham et al., 2014; Farr et al., 2012; Friston et al., 2003; McLaren et al., 2012a; Raz et al., 2014).

Context-dependent connectivity, or the connectivity during different task conditions, has the potential to reveal information about neural and synaptic function and response. Psychophysiological interactions (PPI), the form of context-dependent connectivity used in the present analysis, specifically investigates how one brain region increases or decreases its relationship with another brain region under different contexts (Cisler et al., 2013; Friston et al., 1997; O'Reilly et al., 2012). Generalized psychophysiological interactions (gPPI; McLaren et al., 2012a) assesses how the connectivity changes for each task condition relative to the implicit baseline, usually fixation. This method has been shown to be more sensitive and accurate at estimating the pair-wise connectivity differences between conditions (e.g. novel>repeated) than the standard PPI implemented in SPM software (SPM5/8; Cisler et al., 2013; Gitelman et al., 2003; McLaren et al., 2012a). In the present study, in individuals with mild AD, it was hypothesized that increased accuracy of gPPI analyses may allow the detection of subtle differences in hippocampal seed-whole brain

connectivity that are related to specific tasksupported (context-dependent) cognitive processes.

Context-dependent connectivity approaches are varied and include PPI, dynamic causal modeling and beta-series correlations, but each should be tailored to the question at hand (Friston et al., 2003; Rissman et al., 2004). For example, while dynamic casual modeling has been shown to be more predictive of memory success than simple task activations (Gagnepain et al., 2011), it requires the analysis to be limited to only an *a priori* specified and small set of brain regions(Neufang et al., 2011; Rytsar et al., 2011). Yet, collectively, previous studies support that context-dependent connectivity has the potential to characterize neural correlates of synaptic, neuronal and/or neurovascular integrity as they relate to cognition and behavioral performance.

What remains unknown is whether patterns of context-dependent connectivity, using gPPI, during performance of specific fMRI memory paradigms can capture a representation of neural dysfunction that correlates with specific clinical, cognitive and behavioral impairments. The objective of this study was to determine, in individuals with mild AD dementia, the characteristics of context-dependent hippocampal-whole brain functional connectivity analysis using our fMRI associative memory encoding paradigm in conjunction with performance outside the scanner on clinical and behavioral measures(Diamond et al., 2007; McLaren et al., 2012b; Sperling et al., 2003a). More broadly, the question assessed is whether differences in hippocampal-whole brain connectivity between conditions are related to behavior in AD? We hypothesized that hippocampal connectivity differences between encoding novel face-name pairs (N) and encoding repeated face-name pairs (R) (i.e. the N versus R PPI contrast) in memory performance-related network regions, including the default-mode network, will be associated with cognitive measures in our test battery that better assess episodic memory processes.

2. Materials and methods

2.1. Subjects

Twenty four right-handed, English-speaking subjects meeting National Institute of Neurological and Communicative Disorders and Stroke and the Alzheimer's Disease and Related Disorders Association (NINCDS/ADRDA) criteria for Probable AD(McKhann et al., 1984), with Mini-Mental State Examination (MMSE, see section 2.2 for details) scores between 16–24, and taking a stable-dose of donepezil (Aricept®) treatment 10 mg daily for at least 6 months were enrolled in the study. The subjects were first diagnosed clinically with AD dementia by a clinical neurologist and were subsequently evaluated at one of two University memory disorders units and given the diagnosis of Probable AD by a cognitive neurologist; a diagnosis which was then reviewed and confirmed by the memory disorders unit's consensus committee. Demographics, clinical characteristics and test scores can be found in Table 1. Exclusion criteria included unstable psychiatric or medical illness, severe renal insufficiency, contraindication to MRI, and use of antipsychotic medication in the six months prior to screening. Subjects and caregivers provided informed consent according to the Declaration of Helsinki and with protocols approved by the Partners Healthcare Inc. Institutional Review Board.

2.2. Study Procedure

All subjects first underwent clinical and neuropsychological testing, followed by fMRI, and finally behavioral testing outside the scanner. Neuropsychological and clinical measures included standard measures used in AD clinical trials such as the Mini-Mental State Examination (MMSE; Folstein et al., 1983), AD Assessment Scale - Cognitive Subscale (ADAS-Cog; Pena-Casanova, 1997), Free and Cued Selective Reminding Test (FCSRT; Grober et al., 2000), and Clinical Dementia Rating scale (CDR; Morris, 1993). The data presented here is the baseline data from a longitudinal pharmacological fMRI study in subjects with mild AD dementia. FMRI data from some subjects has been used in previous publications (Atri et al., 2011; Diamond et al., 2007; McLaren et al., 2012b).

MMSE—The MMSE is a standard instrument used to screen global cognitive function in the clinic and for inclusion in dementia clinical trials. Subjects are asked a number of questions that probe a range of cognitive processes including: orientation of time and place; verbal registration of three simple words; attention; delayed recall of the earlier presented words; language (naming; repetition; and following multi-step commands); and visuospatial function (copying of intersecting pentagons). It takes about 7–10 minutes to administer. A higher MMSE score indicates better cognitive performance and scores range from 0 to 30.

ADAS-Cog—The ADAS-Cog is a standard instrument utilized as a primary cognitive outcome measure in AD clinical trials and includes 11 cognitive subscales. In the present study, we focus on the subscales for Word Recall (ADAS-Cog Recall), Delayed Word Recall (ADAS-Cog Delayed Recall) and Word Recognition (ADAS-Cog Recognition) and on the total score (ADAS-Cog Total). In the word recall task, subjects read a list of 10 high-frequency nouns over three trials and are asked to recall as many words as possible after each trial (ADAS-Cog Recall). Immediate recall trials are followed by brief and delayed recall trials (ADAS-Cog Delayed Recall). The number of words not recalled (i.e. number of errors) was used as the measurement values in the regression models. In the word recognition task, subjects are read a list of 12 high-frequency nouns and are then asked to recognize them from a list of the 12 read (presented) nouns and 12 novel (unpresented) nouns. The number of words not recognized or falsely recognized (i.e. number of errors) was used as the measurement values in the regression models. The ADAS-Cog Total score (total number of errors) is the sum of errors on all the subscales. The total time to administer the ADAS-Cog is about 20–25 minutes. Higher ADAS-Cog scores indicate worse cognitive performance and scores range from 0–70 errors.

FCSRT—The FCSRT is utilized in AD behavioral experiments and clinical trails to measure explicit memory performance by using both free recall and cued recall trials to assess storage and retrieval processes. One card at a time, subjects are presented four picture cards, each containing four pictures (for an ultimate total of 16 pictures) and for each card are instructed to name each picture item according to a semantic cue (e.g., “there is a fruit, what is it?”). For each picture card, once the subject names all four items, the card is flipped hiding the items, and the subject is asked to again name the four items on each card she/he had just seen; semantic cueing is provided for any missed item until all four items per card are named in this way. Once all four picture cards (hence all 16 items) have been “learned”,

subjects are asked to freely recall all sixteen items without cueing (free recall), and then are provided verbal semantic cueing for any missed items (i.e., selective reminding). This process is repeated for a total of three trials, with a 20-second interference task (serial subtraction of 3s from 100) between each trial. The sum of correctly freely recalled items across trials (FCSRT Free score) and the sum of both correct free and cued recall items (FCSRT Total score) were used as the measurement values in the regression models. The total administration time of the FCSRT is about 15–20 minute. Higher scores indicate better cognitive performance and scores range from 0–48.

CDR—The CDR is extensively used in clinical dementia research and AD clinical trials to stage dementia severity. The scale is based on a structured clinical interview that includes the assessments of six cognitive and functional domains: memory; orientation; judgment and problem-solving; community affairs; home and hobbies; and personal care. For the present study, we use the CDR sum-of-box score (CDR-sb), which is the sum-total for each of the six CDR domains that are scored from 0–3 (0 = no dementia; 3 = severe dementia severity). The CDR takes about 20 minutes to administer as part of the overall clinical research assessment. Higher CDR-sb scores indicate higher dementia severity and scores range from 0–18.

2.3. MRI Protocol

2.3.1. MRI acquisition—A GE 3T SIGNA (Waukesha, WI) MRI system with a quadrature birdcage head coil was utilized. High-resolution T1-weighted structural imaging utilized a spoiled gradient recalled sequence with repetition time (TR) = 7.25 ms, echo time (TE) = 3 ms, field of view (FOV) = 240 × 240 mm, flip angle (FA)= 7°, matrix = 256 × 256 mm, and 128 sagittal slices with a thickness of 1.33 mm. Functional scans utilized a T2*-weighted gradient-echo echo-planar image blood-oxygen-level-dependent sequence with TR/TE = 2,500/30 ms, FOV = 240 × 240 mm, FA = 90°, matrix = 64 × 64, and 29 oblique coronal slices with a thickness of 5 mm perpendicular to the AC-PC line with a 1 mm gap. Functional scans consisted of 6 task runs, each having 102 time points.

2.3.2. Task Design—This study employs an established block design face-name associative encoding fMRI paradigm that probes the functional neuroanatomical specificity of associative memory encoding processes(Atri et al., 2011; Celone et al., 2006; Diamond et al., 2007; McLaren et al., 2012b; Pihlajamaki and Sperling, 2009; Putcha et al., 2011; Sperling, 2007; Sperling et al., 2003a; Sperling et al., 2002; Sperling et al., 2003b; Sperling et al., 2001). The task consists of three conditions presented in blocks: (*i*) novel face-name pairs, in which unfamiliar faces are paired with first names each shown once (5-sec duration); (*ii*) repeated face-name pairs, in which two face-name pairs are repeatedly alternated during each block; and (*iii*) fixation cross. Subjects are instructed to press a button to indicate whether or not a name fits a face and to remember the pair. A total of 84 novel face-name pairs, each presented once, and 2 repeated face-name pairs, each presented 42 times, were used. After scanning, subjects were asked to freely recall names for faces they recognized as having been presented during scanning and were next asked to identify, in a forced-choice format, the name that was paired with a given face during scanning. The percentage of names correctly recalled was used as the post-scan free recall (FR) measure.

The percentage of names correctly identified in the alternative force-choice format was used as the post-scan forced choice recognition (FCR) measure.

2.4. Image Preprocessing and First-Level Analyses

Images were slice time corrected using AFNI (Medical College of Wisconsin, USA). Then the following pre-processing steps were completed in SPM8 (Wellcome Department of Imaging Neuroscience, University College London, UK): (1) motion corrected; (2) spatially normalized to the MNI EPI template image; (3) re-sampled to 2 mm isotropic voxels; and (4) smoothed with an 8 mm full-width at half maximum Gaussian kernel. General linear models (GLM) were used to derive single subject activations for the novel encoding and repeated encoding blocks(McLaren et al., 2012b). Novel and repeated blocks were separately convolved with a canonical hemodynamic response function to form task regressors. The GLMs included a constant term per run, a high frequency signal filtering (cutoff = 1/260 Hz), motion parameters, and regressors for bad points. Bad points were defined as any of the following: (1) spike in the data that was more than 2.5 standard deviations of the average variation; (2) movement of more than 0.75 mm between TRs; or (3) rotation of more than 1.5 degrees between TRs. Fixation periods were not explicitly modeled.

Automated quality control excluded any imaging run that had >20 bad points (~20% of data), overall motion >3 millimeters, or overall rotation >5 degrees. Quality control also included manually inspecting the raw time series, pre-processed time series (smoothed normalized images) and first-level results. Based on these metrics, no subjects needed to be excluded.

2.5. Generalized Psychophysiological Interaction Analyses

Based on previous work in other populations that suggests high potential for sensitivity and specificity to detect connectivity effects (McLaren et al., 2012a), generalized psychophysiological interaction (gPPI) were used in this sample to compute the context-dependent connectivity of the left posterior hippocampus and the right posterior hippocampus with all other brain voxels in subjects with mild AD. The left posterior hippocampus seed was defined as a 6 millimeter sphere around the peak activity for novel faces greater than fixation (MNI: −20, −32, −2; Sperling et al., 2002). The right posterior hippocampus seed was defined as a 6 millimeter sphere around the peak activity for novel faces greater than fixation (MNI: 24, −28, −6; Sperling et al., 2002).

Implementation of gPPI in this study used the publicly available gPPI Toolbox (http://www.nitrc.org/projects/gppi). This toolbox creates a design matrix with the three sets of columns per run: (1) task regressors formed by convolving the task blocks with the canonical hemodynamic response function; (2) BOLD signal observed in the seed region; and (3) PPI regressors for each task that are formed by separately multiplying the tasks by the deconvolved BOLD signal observed in the seed region, and then convolved with the canonical hemodynamic response function. In the present experiment, there were 5 regressors modeling the BOLD signal per run: (1) novel task regressor; (2) repeated task regressor; (3) BOLD signal in the PPI seed region; (4) novel PPI regressor; and (5) repeated

PPI regressor. The GLMs also included a constant term per run, a high frequency signal filtering (cutoff = 1/260 Hz), motion parameters, and regressors for bad points (see Section 2.4). Following the creation of the design matrix, the gPPI Toolbox estimates the model parameters and computes linear contrasts. In the present study, the linear contrast of novel PPI minus repeated PPI regressor, N-R PPI (i.e. N>R PPI), is calculated and used in the second-level models. The N-R (N>R PPI) contrast computed for each voxel in the brain represents the difference in hippocampal functional connectivity between encoding novel face-name pairs and encoding repeated face-name pairs. We have included the gPPI configuration file (gPPI_AD_config.mat) as a supplemental file.

2.6. Second-Level Analysis: Correlation Between Connectivity Differences and Behavioral Measures

Whole brain linear regression investigated which regions showed a correlation between hippocampal functional connectivity differences and the behavioral measures. The hippocampal connectivity difference between encoding novel face-name pairs and encoding repeated face-name pairs (N-R; N>R PPI), which represents a measure of an individual's ability to modulate connectivity, was entered into the regression models as the dependent variable. Separate models used ADAS-Cog Recall, ADAS-Cog Delayed Recall, ADAS-Cog Recognition, ADAS-Cog Total, FCSRT Free, FCSRT Total, FR, FCR, CDR-sb, and MMSE as independent variables. Each model also included age and education as covariates. Regression results for ADAS-Cog Recall, ADAS-Cog Delayed Recall, ADAS-Cog Recognition, ADAS-Cog Total, and CDR-sb were reversed to make increased (higher) connectivity differences positively correlate with increased (better) performance. Negative regression results are reported as the correlation with the difference in connectivity during encoding repeated face-name pairs and encoding novel face-name pairs (R-N PPI; R>N). Hereafter, all correlations reported are positive correlations. Significant clusters ($p<0.05$) were defined as clusters with at least 174 contiguous voxels (1392 mm^3) attaining $p<0.01$ based on 3dClustSim in AFNI.

2.7. Third-Level Analysis: Connectivity-Behavior Conjunction

To explore the extent of similarity across (e.g. spatial overlap) the different behavioral measures, we thresholded the correlation maps for each regression model separately for the significant N>R PPI and R>N PPI correlations. Each thresholded correlation map was converted to a binary map of 1s and 0s. Then the 10 binary maps for N>R PPI hippocampal connectivity-behavior correlations were summed together to produce a map that indicated how many behavioral tests were significantly correlated with the N>R PPI connectivity differences at each voxel. Finally, the 10 binary maps for R>N PPI correlations were summed together to produce a map that indicated how many behavioral tests were significantly correlated with the R>N PPI connectivity differences at each voxel.

2.8. Third-Level Analysis: Network Distribution of Connectivity-Behavior Effects

Using eight resting state functional network maps (Supplementary Figure 3) defined by Smith et al. (2009)[1] and publicly available (http://fsl.fmrib.ox.ac.uk/analysis/brainmap+rsns/), we counted the number of voxels in each Smith-adapted networks at 3 thresholds: (1) top 25%; (2) top 5%; and (3) top 1% of all correlations, based on t-statistic from the

regression model, within any of these eight Smith-adapted networks, and then divided by the total number of voxels in each network. This process was repeated for each regression model and direction (i.e. N>R PPI and R>N PPI). Selecting a specific number of voxels from each test and correcting for network size allows for a potentially more accurate and robust representation of spatial distributions than the method of counting the number of significant voxels as such counts can be skewed by voxel and cluster thresholds. For each threshold, we tested the distribution for each regression model against a uniform distribution where 25%, 5%, or 1% of every network was above the threshold. We further directly compared the distributions of the correlations of behavioral measures. These two metrics enable interpretations to be made about the networks involved in connectivity-behavior relationships.

2.9. Third-Level Analysis: Hemispheric Connectivity-Behavior Correlation Differences

T-statistics of the partial correlations of connectivity with behavior were converted to equally probable Z-scores for each regression model. The right hippocampal seed region Z-scores were subtracted from the left hippocampal seed region Z-scores. Significant clusters ($p<0.05$) were defined as clusters with at least 174 contiguous voxels (1392 mm^3) attaining $p<0.01$ based on 3dClustSim in AFNI.

3. Results

3.1. Neuropsychological, Clinical, and Behavioral Results

The average ADAS-Cog Total score was 26.15±1.90 (mean ± standard error of the mean) errors, which is consistent with performance in the mildly impaired range. This is consistent with the study inclusion criteria regarding baseline MMSE scores to range of 16–24 (mean 24.04±0.58). The mean CDR-sb was 4.67±0.50, which is also consistent with mild-stage dementia.

The mean number of errors on the ADAS-Cog Recognition test was 6.71±0.66, on the ADAS-Cog Recall test was 5.94±0.35, and on the ADAS-Cog Delayed Recall test was 8.33±0.39. The mean total score on the FCSRT was 30.54±2.78, while the mean score on the free portion (FCSRT Free) was 10.08±1.72 (Table 1).

The mean percentage correct on the post-scan free recall (FR) test was 67%±3.05, indicating that the participants were able to encode the face-name pairs. The mean percentage correct on the post-scan alternative forced-choice (FCR) was 68.75%±3.31, which was substantially better than chance performance of 50%.

3.2. Correlation Between Connectivity Differences and Cognitive/Behavioral Measures

All 10 behavioral measurement regressions revealed at least one significant cluster (Table 2). Most of the significant connectivity-behavior relationships were found with neuropsychological and clinical tests that specifically probe episodic memory function (i.e. FCSRT Free, FCSRT Total, FR, FCR, ADAS-Cog Recall, ADAS-Cog Recognition, and

[1]Networks 1&2 were combined. Networks 9&10 were combined.

ADAS-Cog Delayed Recall). In particular, we observed the most number of correlations (to brain regions) and the strongest correlations with the FCSRT Free test, which is the most difficult episodic memory specific assessment in this test battery. Whereas, very few and generally weaker relationships were observed with global measures such as the CDR-sb and MMSE. The ADAS-Cog Total score had more and stronger relationships than the global measures, but fewer and weaker relationships than the memory subscales of the ADAS-Cog (i.e. ADAS-Cog Recall, ADAS-Cog Recognition, and ADAS-Cog Delayed Recall). These observations support the hypothesis that the flexibility of connectivity during memory encoding is most associated with the ability to perform on tasks of episodic memory. Overall, significant clusters spanned the majority of the brain (Supplementary Figures 1/2, Supplementary Tables 1/2). However, tests of episodic memory function were most associated with the ability to modulate hippocampal connectivity with visual cortices and memory network regions that included the temporal pole, middle temporal gyrus, superior frontal gyrus, supramarginal gyrus and angular gyrus,

The relationship between behavior and the ability to modulate connectivity provides insights into which dynamic connections underlie cognitive test performance. Using Table 2, researchers can identify which connections need to remain dynamic or to increase their dynamic range to improve performance on a given cognitive measure. For example, as an experimental candidate to improve the total score on the FCSRT test, one could target to increase the flexibility of the functional connectivity between the right hippocampus and right angular gyrus.

3.3. Conjunction of Left Hippocampal Seed Connectivity-Behavior Correlations

A number of clusters were observed to be in common among the different behavioral test/measure correlations for the left hippocampal seed connectivity contrasts (i.e. the N and R PPI differences) (Figure 2, Supplementary Figure 1, Table 2). Notably, significant connectivity-behavior spatial overlaps predominately occurred for tests of episodic memory function. In the supramarginal gyrus and rolandic operculum, the correlations for ADAS-Cog Delayed Recall, ADAS-Cog Recognition and FCSRT Free with the N>R PPI contrast spatially overlapped. In the middle cingulate cortex, ADAS-Cog Delayed Recall and CDR-sb correlations with N>R PPI spatially overlapped. In the right anterior temporal lobe, significant correlations of N>R PPI with ADAS-Cog Delayed Recall and FCSRT Free spatially overlapped. In the left anterior temporal lobe, significant correlations were observed with the ADAS-Cog Recognition, FCSRT Free, and FCR for N>R PPI (Figure 1).

In the right orbital frontal cortex, significant correlations for R>N PPI with FCSRT Free and ADAS-Cog Recognition spatially overlapped. In the right hippocampus/parahippocampus and right temporal pole, significant correlations for R>N PPI with FCSRT Total and ADAS-Cog Recognition spatially overlapped. Spatial overlap was also observed in the cerebellum.

3.4. Conjunction of Right Hippocampal Seed Connectivity-Behavior Correlations

A number of clusters were also in common among the behavioral correlations for the right hippocampal seed connectivity contrasts (Figure 2, Supplementary Figure 2, Table 2). In the left calcarine sulcus, significant correlations for N>R PPI with ADAS-Cog Recognition,

FCSRT Free and FCR spatially overlapped (Figure 1). In the right angular gyrus, middle occipital gyrus, and middle temporal gyrus, significant correlations for N>R PPI with ADAS-Cog Recall, FCSRT Free and FCSRT Total spatially overlapped. Spatial overlap between FCSRT Free and FCSRT correlations with N>R PPI was also observed in other parts of the posterior occipital lobe.

In the right middle frontal gyrus and precentral gyrus, significant correlations for R>N PPI with ADAS-Cog Total, FCSRT Total, FR, and MMSE spatially overlapped. This overlap extended into the superior frontal gyrus for at least 3 of 4 regressions. In the left posterior and middle cingulate cortex, significant correlations for R>N PPI with ADAS-Cog Recognition and FR spatially overlapped. In the right supramarginal gyrus and postcentral gyrus, significant correlations for R>N PPI with ADAS-Cog Total and CDR-sb spatially overlapped. Notably, the spatial overlap of R>N PPI correlations were on more global measures of cognition compared to the N>R PPI effects, which more closely related to measures of episodic memory.

3.5. Dynamically Overlapping Task-Specific Intrinsic Networks

To follow up the observation of spatial similarity and disparity across the behavioral test/measure correlations, we sought to statistically test if these connectivity-behavior relationships were different from each other and spatially non-random across intrinsic networks. The proportion of each Smith-adapted network (Smith et al., 2009) that had voxels in the top 1%, 5%, or 25% of associations is reported in Supplementary Tables 5–7 (Figure 3, Supplementary Figures 4–9). In general, irrespective of the threshold (1 vs 5 vs 25%), N>R PPI relationships were more commonly observed in visual and default-mode networks; while R>N PPI relationships were more commonly observed in the executive and frontoparietal networks. In some instances, significant portions of a network contained both N>R PPI and R>N PPI correlations for the same behavioral task/clinical measure indicating potential subdivisions in each network (Figure 3, Supplementary Figures 4–9). The graphs suggested that, irrespective of threshold, there are dissociations amongst the correlations with the behavioral/clinical measures; these were confirmed for all spatial patterns ($p<0.001$ bonferonni-corrected, Supplementary Tables 8–10). We also confirmed that the spatial distribution of voxels above the selected thresholds was not uniform across the Smith-adapted cognitive networks ($p<0.001$ bonferonni-corrected). Finally, while substantial similarities existed, overall the spatial patterns were different between left and right hippocampal seed regions.

3.6. Differences between the connectivity-behavior correlations of the left and right hippocampal seeds

A number of regions had different correlations with behavior between the two posterior hippocampal seed regions (Supplementary Table 11). Compared to the findings for each seed region, the connectivity-behavior differences, when comparing right and left hippocampal seeds, were not associated with a specific measure type but were different for both tests of episodic memory and measures of global cognition. These findings support laterality in functional connectivity profiles between the left and right hippocampus during episodic memory encoding.

4. Discussion

In this study we applied gPPI to assess the nature of fMRI task-based context-dependent connectivity's relationship with cognitive, clinical and behavioral assessments. As an illustration of gPPI's potential utility as a tool to explore brain context-dependent connectivity-behavior relationships, these relationships were characterized in patients with mild AD during the performance of a well-studied and ecologically valid task, the encoding of novel and repeated face-name pairs, in relation to performance on post-scan memory tests and to scores on highly relevant assessments of cognitive/clinical function performed outside the scanner. This is the first study to apply gPPI to assess functional connectivity in the context of delineating brain connectivity-behavior relationships. Results revealed performance on behavioral and clinical measures of episodic memory and global cognition are correlated, in unique spatial patterns within and across intrinsic brain networks, with the ability to modulate connectivity in response to encoding novel and repeated face-name pairs. Furthermore, significantly greater and more complex relationships were observed using gPPI than had been previously observed in patients with AD using fMRI activity-behavior regression analysis(Diamond et al., 2007).

In support of our *a priori* hypothesis, tests of episodic memory function were associated with the ability to modulate hippocampal connectivity within memory network regions. The observed regions included the temporal pole, middle temporal gyrus, superior frontal gyrus, supramarginal gyrus and angular gyrus. Additionally, significant connectivity relationships were observed with regions that support visual integration, facial recognition and cognitive control. The hippocampal connectivity patterns revealed encoding novel face-name and repeated face-name pair connectivity differences both within the network containing the seed as well as throughout other brain networks (Figure 3, Table 2). In particular, increased ability to modulate connectivity related to behavior was found in the visual (within-network connectivity), default-mode (out-of-network connectivity), executive control (out-of-network) and frontoparietal (out-of-network connectivity) networks. For referential purposes, in this paper we utilized the atlas of resting state functional networks from Smith et al. (2009) to classify the intrinsic network related to the location of the seed regions based on the winner take all approach. Based on this classification scheme, the a priori defined posterior hippocampal seeds fell predominantly within the medial and lateral visual networks. In a "winner take all" binary categorization, whether a hippocampal region is classified to fall within the visual or another network is likely most driven by context-specific functionality. Previous work from our lab (Ward et al., 2013) and by others (Hellyer et al., 2014; Kahn et al., 2008) supports the observation that at least some hippocampal regions are functionally apart from the default-mode network. Hence, the results presented here that demonstrate hippocampal seed-connectivity modulation with default-mode network and other regions, are interpreted, by definition, to represent detection of out-of-network connectivity. This is not to suggest that the hippocampus or subdivisions of the hippocampus are not functionally connected to other networks during the performance of specific memory tasks and under certain rest conditions. More broadly, these findings reveal, even in patients with AD, significant fMRI task-based connectivity-behavior relationships that are unique and span across several brain networks, particularly in relation

to performance on measures of episodic memory. These findings further corroborate the idea that brain regions are not part of single networks but are part of multiple networks that have preferred connections or ‘coordinated states’. In other words, regions that are part of one network during fMRI resting state may become, more or less, coordinated with subparts of the network (within-network changes) and subparts of other networks (out-of-network changes) (Hellyer et al., 2014).

4.1. A cognitive perspective of context-dependent connectivity: ‘coordinated states’

This study and others indicate how networks interact to subserve a multitude of cognitive processes. Additionally observations from this study provide evidence to support that cognitive task-specific profiles spatially span different networks, and that the temporal dynamics of overlapping connectivity should change to yield a different connectivity-task-specific profile when the task changes. Both anatomical and resting-state connectivity studies have characterized a core set of brain networks (Beckmann et al., 2005; Fox et al., 2005; Greicius et al., 2003; Hagmann et al., 2008; Laird et al., 2011; Seeley et al., 2009; Smith et al., 2009). While these core networks subserve cognition (Laird et al., 2011; Seeley et al., 2007), they do not necessitate that cognitive processes only occur within a network, and empirical evidence does not support such an absolute interpretation (Brier et al., 2012; Kelly et al., 2008). In particular, Kelly and colleagues (2008) observed that out-of-network connectivity was more predictive of behavior than within-network connectivity. Even at the electrophysiological level, recordings in cats have demonstrated that task-on and task-off networks change between uncorrelated and anti-correlated states (Popa et al., 2009). The predominant resting state can be thought of as a particular ‘coordinated state’ within and between networks. As the brain becomes engaged in a particular cognitive process, it transitions into another metastable ‘coordinate state’ (Bressler and Kelso, 2001). Importantly, the brain can rapidly switch between these metastable states to perform different cognitive functions (Andrews-Hanna et al., 2010a; Cole et al., 2013). The transition from one state to another enables the brain to integrate information from a multitude of brain regions. It can therefore be posited that these stastes can: (1) change with age (Addis et al., 2010); (2) change with disease states (Greicius et al., 2004; Hedden et al., 2009); (3) change with pharmacological modulation (Abler et al., 2012; Schon et al., 2005; Sperling et al., 2002); and (4) recruit subcomponents of different brain networks (Andrews-Hanna et al., 2010b; Gour et al., 2011; Kim, 2012; Sepulcre et al., 2010). As a result of a predominant state, the default-mode network can act as a sink to integrate internal and external events – or episodic information.

Drawing upon the recent finding by Ward and colleagues (2013), which supports that the hippocampus is not “intrinsically and implicitly” part of the default-mode network, we propose that: (1) there is a rapid shift to a state when, due to environmental or task demands, the hippocampus becomes transiently “extrinsically and explicitly” connected to the default-mode network, and (2) this dynamic underlies episodic memory encoding. Recent work has indicated that local and distant connectivity differs between the resting and task states (Sepulcre et al., 2010) and can rapidly change between different task states (Cole et al., 2013; Hellyer et al., 2014). Additionally, Cole and colleagues demonstrated that the frontoparietal network, at least for decision-making tasks, has the most variance between

tasks in its connectivity with other brain regions (2013). Akin to other seed-based resting connectivity methods, gPPI is likely to be multi-synaptic (Vincent et al., 2007).

4.2. Relationships to Other Brain-Behavior Studies of Memory Performance in AD

Compared to the fMRI task-activity findings presented in Diamond et al. (2007), the regions identified here, using task-based connectivity-behavior methods, are different. This observation indicates that task-based connectivity and activation analyses may provide complementary information about cognitive processing in AD. Frontal areas are more active during episodic memory tasks in individuals with AD (Grady et al., 2003a; Pariente et al., 2005; Sperling et al., 2003b) and task activity in these regions is correlated with memory performance (Diamond et al., 2007). However, medial temporal lobe integrity is still essential to affect effective episodic memory processing, and the loss of medial temporal lobe connections to subcortical or cortical areas is also known to impair relational memory (Dusek and Eichenbaum, 1997). Thus, understanding how these connections effectively change during performance of memory processes may also be important to understanding the potential compensatory mechanisms that might remain available in individuals with AD. It may also be essential to discern which connections are reversibly versus irreversibly functionally damaged, in addition to connections that are structurally damaged.

While atrophy represents a structural change, it might not be fully indicative of changes in function-behavior relationships. For example, it has been observed that as the number of synapses are reduced, the size and number of connections at a synapse might increase (Scheff and Price, 1993). Nevertheless, structural studies provide evidence of potential functional changes. Carmichael and colleagues (Carmichael et al., 2012) recently identified two AD-related patterns of atrophy in individuals with mild cognitive impairment. The first pattern revealed coordinated atrophy across posterior nodes of the default-mode network, while the second pattern largely represented atrophy in the medial temporal lobe. Their observations provide further support that structural changes in AD do not uniformly encompass entire resting brain/intrinsic networks; nor are they isolated to a single network. As such, the maintenance of cognitive abilities in individuals with AD need not be limited to entire networks(Andrews-Hanna et al., 2010b) or isolated to single networks(Grady et al., 2003b; Wang et al., 2006). Interestingly, the most consistent effects observed here were across behavioral measures in the posterior nodes of the default-mode network. This further demonstrates that though posterior default-mode network regions, which are involved in episodic memory, are anatomically damaged in AD they retain functional importance to modulate connectivity-behavior relationships.

These context-dependent connectivity results share important similarities to both functional and structural brain-behavior relationships previously observed and conceptualized (Figure 2, Table 2). For example, a recent study revealed significant correlations between performance on the FCSRT and grey matter volume in the left supramarginal gyrus, anterior cerebellum, and left superior temporal gyrus (Rami et al., 2012b). The latter area is similar to the region observed here that shows a strong correlation between the ability to modulate connectivity for encoding novel versus repeated face-name pairs and better performance on FCSRT. In the present study, we also observed correlations with posterior medial parietal

areas; these areas tend to show task activity differences earlier in the disease process relative to the lateral temporal lobe areas (Rami et al., 2012a; Sperling et al., 2003b). Evidence from other brain-behavior studies and this study provide good support for the more general concept that structure-function relationships that support cognitive tasks in AD can be uniquely spatio-temporally distributed within and between brain networks.

4.3. Potential Application to Clinical Trials: AD as an illustrative example

Our ability to understand the functional integrity of brain networks is becoming increasingly important to better interpret both clinical trial data and underlying disease progression. It has been proposed that it is initial neuronal dysfunction that triggers the accumulation of amyloid (Cirrito et al., 2005; Jagust and Mormino, 2011; Sperling et al., 2009). While increases in amyloid plaques or decreases in amyloid in the CSF are considered hallmark pathological features of AD, recent and historical studies indicate that AD pathology is not necessary for clinical diagnosis (Mayeux et al., 1998). At issue may not be whether these patients are misdiagnosed or whether amyloid is a by-product of the disease and not yet detected (Hyman et al., 2012), but whether individuals diagnosed with probable AD have a similar phenotype. The development of AD therapeutics should target both the presumed pathologies and the maintenance or enhancement of the connectivity associated with better cognitive, functional and behavioral profiles in patients with AD. It is therefore prudent that such therapeutic approaches not solely depend on binarized biomarkers for the presence/absence of presumed AD pathologies but consider phenotypic “dysfunction” patterns characterized by the AD syndrome. In this light, probes of the functional integrity and the capacity to modulate cognitive and task-specific systems are complementary and, perhaps, equally important as amyloid load as markers of disease in patients with probable AD.

The utilization of imaging biomarkers is not a replacement for neuropsychological testing, but rather a complement to them. The significant correlations observed in the present study provide evidence that important variance related to cognitive performance in AD is being captured. It also provides support that this particular imaging biomarker, context-dependent connectivity implemented in the form of gPPI, may potentially further capture a unique variance that could be leveraged in early phase trials. Thus, the goal is not to replace neuropsychological tests, but to develop imaging biomarkers that, when combined in integrated models with other variables (including neuropsychological measures), yield greater explanatory power, particularly for clinical changes over time. In particular, fMRI may potentially reveal signals of effects at the neuronal, neurovascular or synaptic/local field potential levels that are likely to be present at much earlier points than changes in behavior; such signals could help guide drug discovery, dose selection, and therapeutic trial efforts. The results presented here, coupled with prior evidence that quantify fMRI effects in AD, lend support to further exploratory investigation of fMRI methods in early phase/proof of concept AD trials(Atri et al., 2011; Putcha et al., 2011).

In showing strong relationships between the ability to modulate connectivity and forced-choice recognition, a direct measure of performance on this task, we further validate this face-name encoding paradigm in understanding the integrity of the episodic memory network in AD. Furthermore, the present study identifies the posterior nodes of the default-

mode network and frontoparietal network as key regions that have potential as functional biomarkers in clinical trials. In the default-mode network, these key areas are the lateral temporal lobe and precuneus. In the frontoparietal network, the key areas are supramarginal gyrus, inferior parietal lobule, inferior temporal gyrus, middle frontal gyrus and superior parietal lobule. It should be noted that large portions of the supramarginal gyrus and inferior parietal lobule also fall in the posterior nodes of the default-mode network. Cognitive, behavioral, and/or pharmacological interventions may utilize the present hippocampal task-PPI method to focus on increasing or maintaining the dynamic range of connectivity between these target regions and the hippocampus.

4.4. Future Directions and Caveats

The present results provide evidence of additional cross-sectional fMRI-task relationships that complement earlier work (Diamond et al., 2007). However, these results do not provide an indication of how hippocampal-whole brain connectivity-behavior patterns may change over time. They also do not quantify the test-retest reliability and sensitivity of gPPI for detecting various effect sizes, as has already been shown in task activation studies in AD (Atri et al., 2011; McLaren et al., 2012b). Thus, future work is aimed at: (1) investigating the longitudinal relationships between task-based connectivity and behavior; and (2) assessing the test-retest reliability and power analysis for gPPI studies.

Additionally, in this initial gPPI study we utilized posterior hippocampal seeds based on our earlier work with task-related BOLD activity analysis of this paradigm (Sperling et al., 2002). While we observed numerous strong connectivity-behavior associations with this choice of hippocampal seeds, this does not necessarily represent the connectivity relationships for the entire hippocampus or the optimal hippocampal seed locations that would reveal the strongest connectivity-behavior association in the context of gPPI analysis. For example, choosing a more anterior hippocampal seed may have resulted in greater associations within the default-mode network. Future studies can assess optimization of seed placements in the context of identifying the strongest connectivity-behavior associations for any targeted network.

This study also utilized an imaging sequence that essentially had 6mm thick slices, which may have reduced the ability to detect smaller and more focal changes. However, given the observed large cluster sizes, the robustness of the correlations and the investigations of the spatial distribution of connectivity at different thresholds across intrinsic networks, it is unlikely that utilizing lower slice thicknesses would have changed the major conclusions of this study. Nevertheless, future studies should use slices of 4 mm or less in thickness.

5. Conclusions

The observation that task-based connectivity during an associative-encoding task bears unique and significant relationships within and between intrinsic brain networks to task performance on measures of episodic memory and global cognition, even in subjects with mild AD, supports the potential utility of gPPI to characterize complex context-dependent connectivity-behavior relationships; it also backs further exploration of task-based connectivity-fMRI as a functional biomarker of behavior. Hippocampal-whole brain

connectivity-behavior relationships were not isolated to single networks, but spanned multiple brain networks and were unique for each behavioral measure. Importantly, these connectivity-behavioral performance profiles were more widespread than previously observed in task activations studies, thus providing complementary information about how brain function might underlie cognition. Numerous significant hippocampal connectivity relationships with behavioral performance were observed in our small sample, which suggests the engagement of 'coordinated states'. The correlations between PPI differences and behavioral measures reveal complex patterns of connectivity underlying cognitive processes that support performance of specific tasks and shared mental functions. Using this face-name encoding paradigm, the ability to modulate connectivity during encoding of novel versus repeated face-name pairs between the hippocampus and nodes of the memory network was most strongly and consistently related to better episodic memory performance in subjects with AD. Different regions showed different hippocampal connectivity-behavior relationships. While the particulars of these results require further validation in larger and longitudinal studies, nonetheless, the general observations here provide evidence that the capacity to gauge the functional neuroanatomy that supports task-specific performance can be enhanced by integrative multivariate modeling approaches that simultaneously combine structural, functional and behavioral contexts.

Supplementary Material

Refer to Web version on PubMed Central for supplementary material.

Acknowledgements

Dr. Kim Celone, Ms. Amy DeLuca, Dr. Kristina DePeau, Dr. Eli Diamond, Dr. Saul Miller, Dr. Meghan Mitchell, Dr. Jacqueline O'Brien, Ms. Kelly O'Keefe, Dr. Maija Pihlamajaki, Ms. Sarah Rastegar, Dr. Dorene Rentz, Ms. Sibyl Salisbury, and Dr. Meghan Searl provided assistance with data collection. We also appreciate the assistance from the clinical, neuroimaging (Dr. Bradford Dickerson), education and administrative cores (Dr. Liang Yap) of the Massachusetts AD Research Center. Dr. John Growdon (Massachusetts General Hospital Memory Disorders Unit & Massachusetts AD Research Center) provided significant assistance with recruitment of participants, obtaining space, resources, and guidance. Dr. Bruce Rosen (MGH-Harvard-MIT Martinos Center for Biomedical Imaging) provided guidance, space, and resources for this research. We wish to thank the anonymous reviewers and the journal editor for providing thoughtful comments and suggestions to improve the manuscript. Finally, and most importantly, we express our deep gratitude for the commitment of the patients, family members, and caregivers without whose generous contribution and dedication this research would not be possible. The content is solely the responsibility of the authors and does not necessarily represent the official views of the National Institute on Aging, the National Institutes of Health, the Department of Veterans Affairs or the United States Government.

Funding

The study was supported by: NIA National Institute on Aging grants: K23 AG027171 (Dr. Atri), F32 AG042228 (Dr. McLaren), RO1 AG027435 (Dr. Sperling), and P01 AG036694 (Dr. Sperling); The Harvard-Massachusetts Institute of Technology Health Sciences & Technology Pfizer-Merck Clinical Investigator Training Program (Dr. Atri); the NIH National Institutes of Health loan repayment program (Dr. Atri); Investigator-Initiated Research Grants from Forest Pharmaceuticals and The Harvard Center for Neurodegeneration & Repair; the Clinical, Neuroimaging, and Statistics Cores of the Massachusetts AD Research Center (NIA National Institute on Aging grant P50 AG05134 to Drs. Growdon and Hyman); and the Geriatric Research, Education and Clinical Center (GRECC) at the Edith Nourse Rogers Memorial (ENRM) Veterans Administration Bedford Medical Center. The views expressed in this article are those of the authors and do not necessarily reflect the position or policy of the Department of Veterans Affairs, the National Institutes of Health or the United States government. Less than 30% of the funds for data collection were from an Investigator-Initiated Research Grant from Forest Research Institute.

Abbreviations

AD	Alzheimer’s disease
ADAS-Cog	AD Assessment Scale - Cognitive Subscale
CDR	clinical dementia rating
CDR-sb	CDR Sum-of-Boxes
FCSRT	Free and Cued Selective Reminding Test
FCR	post-scan forced-choice recognition
FR	post-scan free recall
GLM	General linear models
gPPI	generalized psychophysiological interactions
MMSE	Mini-Mental State Examination
N>R PPI	connectivity difference between encoding novel face-name and repeated face-name pairs
NINCDS/ADRDA	National Institute of Neurological and Communicative Disorders and Stroke and the Alzheimer's Disease and Related Disorders Association
PPI	psychophysiological interactions
R>N PPI	connectivity difference between encoding repeated face-name and novel face-name pairs

References

Abler B, Grön G, Hartmann A, Metzger C, Walter M. Modulation of Frontostriatal Interaction Aligns with Reduced Primary Reward Processing under Serotonergic Drugs. J Neurosci. 2012; 32:1329–1335. [PubMed: 22279217]

Addis DR, Leclerc CM, Muscatell KA, Kensinger EA. There are age-related changes in neural connectivity during the encoding of positive, but not negative, information. Cortex. 2010; 46:425–433. [PubMed: 19555933]

Andrews-Hanna JR, Reidler JS, Huang C, Buckner RL. Evidence for the default network's role in spontaneous cognition. J Neurophysiol. 2010a; 104:322–335. [PubMed: 20463201]

Andrews-Hanna JR, Reidler JS, Sepulcre J, Poulin R, Buckner RL. Functional-anatomic fractionation of the brain's default network. Neuron. 2010b; 65:550–562. [PubMed: 20188659]

Atri A, O'Brien JL, Sreenivasan A, Rastegar S, Salisbury S, Deluca AN, O'Keefe KM, Laviolette PS, Rentz DM, Locascio JJ, Sperling RA. Test-retest reliability of memory task functional magnetic resonance imaging in Alzheimer disease clinical trials. Arch Neurol. 2011; 68:599–606. [PubMed: 21555634]

Balthazar ML, Pereira FR, Lopes TM, da Silva EL, Coan AC, Campos BM, Duncan NW, Stella F, Northoff G, Damasceno BP, Cendes F. Neuropsychiatric symptoms in Alzheimer's disease are related to functional connectivity alterations in the salience network. Hum Brain Mapp. 2014; 35:1237–1246. [PubMed: 23418130]

Beckmann CF, DeLuca M, Devlin JT, Smith SM. Investigations into resting-state connectivity using independent component analysis. Philosophical Transactions of the Royal Society B: Biological Sciences. 2005; 360:1001–1013.

Biswal B, Yetkin FZ, Haughton VM, Hyde JS. Functional connectivity in the motor cortex of resting human brain using echo-planar MRI. Magn Reson Med. 1995; 34:537–541. [PubMed: 8524021]

Bressler SL, Kelso JA. Cortical coordination dynamics and cognition. Trends Cogn Sci. 2001; 5:26–36. [PubMed: 11164733]

Brier MR, Thomas JB, Snyder AZ, Benzinger TL, Zhang D, Raichle ME, Holtzman DM, Morris JC, Ances BM. Loss of intranetwork and internetwork resting state functional connections with Alzheimer's disease progression. J Neurosci. 2012; 32:8890–8899. [PubMed: 22745490]

Carmichael O, McLaren DG, Tommet D, Mungas D, Jones RN. Coevolution of brain structures in amnestic mild cognitive impairment. Neuroimage. 2012

Celone KA, Calhoun VD, Dickerson BC, Atri A, Chua EF, Miller SL, DePeau K, Rentz DM, Selkoe DJ, Blacker D, Albert MS, Sperling RA. Alterations in memory networks in mild cognitive impairment and Alzheimer's disease: an independent component analysis. J Neurosci. 2006; 26:10222–10231. [PubMed: 17021177]

Chatham CH, Frank MJ, Badre D. Corticostriatal output gating during selection from working memory. Neuron. 2014; 81:930–942. [PubMed: 24559680]

Cirrito JR, Yamada KA, Finn MB, Sloviter RS, Bales KR, May PC, Schoepp DD, Paul SM, Mennerick S, Holtzman DM. Synaptic Activity Regulates Interstitial Fluid Amyloid-β Levels In Vivo. Neuron. 2005; 48:913–922. [PubMed: 16364896]

Cisler JM, Bush K, Steele JS. A Comparison of Statistical Methods for Detecting Context-Modulated Functional Connectivity in fMRI. Neuroimage. 2013

Cole MW, Reynolds JR, Power JD, Repovs G, Anticevic A, Braver TS. Multi-task connectivity reveals flexible hubs for adaptive task control. Nat Neurosci. 2013; 16:1348–1355. [PubMed: 23892552]

Damoiseaux JS, Prater KE, Miller BL, Greicius MD. Functional connectivity tracks clinical deterioration in Alzheimer's disease. Neurobiol Aging. 2012; 33:828, e819–e830. [PubMed: 21840627]

DeYoe EA, Bandettini P, Neitz J, Miller D, Winans P. Functional magnetic resonance imaging (FMRI) of the human brain. J Neurosci Methods. 1994; 54:171–187. [PubMed: 7869750]

Diamond EL, Miller S, Dickerson BC, Atri A, DePeau K, Fenstermacher E, Pihlajamaki M, Celone K, Salisbury S, Gregas M, Rentz D, Sperling RA. Relationship of fMRI activation to clinical trial memory measures in Alzheimer disease. Neurology. 2007; 69:1331–1341. [PubMed: 17893294]

Dolcos F, Iordan AD, Kragel J, Stokes J, Campbell R, McCarthy G, Cabeza R. Neural correlates of opposing effects of emotional distraction on working memory and episodic memory: an event-related FMRI investigation. Front Psychol. 2013; 4:293. [PubMed: 23761770]

Dusek JA, Eichenbaum H. The hippocampus and memory for orderly stimulus relations. Proc Natl Acad Sci U S A. 1997; 94:7109–7114. [PubMed: 9192700]

Ewbank MP, Lawrence AD, Passamonti L, Keane J, Peers PV, Calder AJ. Anxiety predicts a differential neural response to attended and unattended facial signals of anger and fear. Neuroimage. 2009; 44:1144–1151. [PubMed: 18996489]

Farr OM, Hu S, Zhang S, Li CS. Decreased saliency processing as a neural measure of Barratt impulsivity in healthy adults. Neuroimage. 2012; 63:1070–1077. [PubMed: 22885245]

Folstein MF, Robins LN, Helzer JE. The Mini-Mental State Examination. Arch Gen Psychiatry. 1983; 40:812. [PubMed: 6860082]

Fox MD, Corbetta M, Snyder AZ, Vincent JL, Raichle ME. Spontaneous neuronal activity distinguishes human dorsal and ventral attention systems. Proc Natl Acad Sci U S A. 2006; 103:10046–10051. [PubMed: 16788060]

Fox MD, Snyder AZ, Vincent JL, Corbetta M, Van Essen DC, Raichle ME. The human brain is intrinsically organized into dynamic, anticorrelated functional networks. Proceedings of the National Academy of Sciences of the United States of America. 2005; 102:9673–9678. [PubMed: 15976020]

Friston KJ, Buechel C, Fink GR, Morris J, Rolls E, Dolan RJ. Psychophysiological and modulatory interactions in neuroimaging. Neuroimage. 1997; 6:218–229. [PubMed: 9344826]

Friston KJ, Frith CD, Turner R, Frackowiak RS. Characterizing evoked hemodynamics with fMRI. Neuroimage. 1995a; 2:157–165. [PubMed: 9343598]

Friston KJ, Harrison L, Penny W. Dynamic causal modelling. Neuroimage. 2003; 19:1273–1302. [PubMed: 12948688]

Friston KJ, Holmes AP, Poline JB, Grasby PJ, Williams SC, Frackowiak RS, Turner R. Analysis of fMRI time-series revisited. Neuroimage. 1995b; 2:45–53. [PubMed: 9343589]

Gagnepain P, Henson R, Chételat G, Desgranges B, Lebreton K, Eustache F. Is neocortical-hippocampal connectivity a better predictor of subsequent recollection than local increases in hippocampal activity? New insights on the role of priming. Journal of Cognitive Neuroscience. 2011; 23:391–403. [PubMed: 20146612]

Gitelman DR, Penny WD, Ashburner J, Friston KJ. Modeling regional and psychophysiologic interactions in fMRI: the importance of hemodynamic deconvolution. Neuroimage. 2003; 19:200–207. [PubMed: 12781739]

Gour N, Ranjeva JP, Ceccaldi M, Confort-Gouny S, Barbeau E, Soulier E, Guye M, Didic M, Felician O. Basal functional connectivity within the anterior temporal network is associated with performance on declarative memory tasks. Neuroimage. 2011; 58:687–697. [PubMed: 21722740]

Grady CL, McIntosh AR, Beig S, Keightley ML, Burian H, Black SE. Evidence from functional neuroimaging of a compensatory prefrontal network in Alzheimer's disease. J Neurosci. 2003a; 23:986–993. [PubMed: 12574428]

Grady CL, McIntosh AR, Beig S, Keightley ML, Burian H, Black SE. Evidence from functional neuroimaging of a compensatory prefrontal network in Alzheimer's disease. J Neurosci. 2003b; 23:986–993. [PubMed: 12574428]

Greicius MD, Krasnow B, Reiss AL, Menon V. Functional connectivity in the resting brain: a network analysis of the default mode hypothesis. Proceedings of the National Academy of Sciences of the United States of America. 2003; 100:253–258. [PubMed: 12506194]

Greicius MD, Srivastava G, Reiss AL, Menon V. Default-mode network activity distinguishes Alzheimer's disease from healthy aging: evidence from functional MRI. Proc Natl Acad Sci U S A. 2004; 101:4637–4642. [PubMed: 15070770]

Grober E, Lipton RB, Hall C, Crystal H. Memory impairment on free and cued selective reminding predicts dementia. Neurology. 2000; 54:827–832. [PubMed: 10690971]

Hagmann P, Cammoun L, Gigandet X, Meuli R, Honey CJ, Wedeen VJ, Sporns O. Mapping the structural core of human cerebral cortex. Plos Biology. 2008; 6:e159. [PubMed: 18597554]

Hedden T, Van Dijk KRA, Becker JA, Mehta A, Sperling RA, Johnson KA, Buckner RL. Disruption of Functional Connectivity in Clinically Normal Older Adults Harboring Amyloid Burden. J Neurosci. 2009; 29:12686–12694. [PubMed: 19812343]

Hellyer PJ, Shanahan M, Scott G, Wise RJ, Sharp DJ, Leech R. The control of global brain dynamics: opposing actions of frontoparietal control and default mode networks on attention. J Neurosci. 2014; 34:451–461. [PubMed: 24403145]

Hyman BT, Phelps CH, Beach TG, Bigio EH, Cairns NJ, Carrillo MC, Dickson DW, Duyckaerts C, Frosch MP, Masliah E, Mirra SS, Nelson PT, Schneider JA, Thal DR, Thies B, Trojanowski JQ, Vinters HV, Montine TJ. National Institute on Aging-Alzheimer's Association guidelines for the neuropathologic assessment of Alzheimer's disease. Alzheimers Dement. 2012; 8:1–13. [PubMed: 22265587]

Jagust WJ, Mormino EC. Lifespan brain activity, beta-amyloid, and Alzheimer's disease. Trends Cogn Sci. 2011; 15:520–526. [PubMed: 21983147]

Kahn I, Andrews-Hanna JR, Vincent JL, Snyder AZ, Buckner RL. Distinct cortical anatomy linked to subregions of the medial temporal lobe revealed by intrinsic functional connectivity. J Neurophysiol. 2008; 100:129–139. [PubMed: 18385483]

Kelly AM, Uddin LQ, Biswal BB, Castellanos FX, Milham MP. Competition between functional brain networks mediates behavioral variability. Neuroimage. 2008; 39:527–537. [PubMed: 17919929]

Kim H. A dual-subsystem model of the brain's default network: self-referential processing, memory retrieval processes, and autobiographical memory retrieval. Neuroimage. 2012; 61:966–977. [PubMed: 22446489]

Laird AR, Fox PM, Eickhoff SB, Turner JA, Ray KL, McKay DR, Glahn DC, Beckmann CF, Smith SM, Fox PT. Behavioral interpretations of intrinsic connectivity networks. Journal of Cognitive Neuroscience. 2011; 23:4022–4037. [PubMed: 21671731]

Li N, Ma N, Liu Y, He XS, Sun DL, Fu XM, Zhang X, Han S, Zhang DR. Resting-state functional connectivity predicts impulsivity in economic decision-making. J Neurosci. 2013; 33:4886–4895. [PubMed: 23486959]

Mayeux R, Saunders AM, Shea S, Mirra S, Evans D, Roses AD, Hyman BT, Crain B, Tang MX, Phelps CH. Utility of the apolipoprotein E genotype in the diagnosis of Alzheimer's disease. Alzheimer's Disease Centers Consortium on Apolipoprotein E and Alzheimer's Disease. N Engl J Med. 1998; 338:506–511. [PubMed: 9468467]

McKhann G, Drachman D, Folstein M, Katzman R, Price D, Stadlan EM. Clinical diagnosis of Alzheimer's disease: report of the NINCDS-ADRDA Work Group under the auspices of Department of Health and Human Services Task Force on Alzheimer's Disease. Neurology. 1984; 34:939–944. [PubMed: 6610841]

McLaren DG, Ries ML, Xu G, Johnson SC. A generalized form of contextdependent psychophysiological interactions (gPPI): a comparison to standard approaches. Neuroimage. 2012a; 61:1277–1286. [PubMed: 22484411]

McLaren DG, Sreenivasan A, Diamond EL, Mitchell MB, Van Dijk KR, Deluca AN, O'Brien JL, Rentz DM, Sperling RA. Tracking cognitive change over 24 weeks with longitudinal functional magnetic resonance imaging in Alzheimer's disease. Neurodegener Dis. 2012b; 9:176–186. [PubMed: 22456451]

Morris JC. The Clinical Dementia Rating (CDR): current version and scoring rules. Neurology. 1993; 43:2412–2414. [PubMed: 8232972]

Neufang S, Akhrif A, Riedl V, Forstl H, Kurz A, Zimmer C, Sorg C, Wohlschlager AM. Disconnection of frontal and parietal areas contributes to impaired attention in very early Alzheimer's disease. J Alzheimers Dis. 2011; 25:309–321. [PubMed: 21422523]

O'Reilly JX, Woolrich MW, Behrens TE, Smith SM, Johansen-Berg H. Tools of the trade: psychophysiological interactions and functional connectivity. Soc Cogn Affect Neurosci. 2012; 7:604–609. [PubMed: 22569188]

Pariente J, Cole S, Henson R, Clare L, Kennedy A, Rossor M, Cipoloti L, Puel M, Demonet JF, Chollet F, Frackowiak RS. Alzheimer's patients engage an alternative network during a memory task. Ann Neurol. 2005; 58:870–879. [PubMed: 16315273]

Pena-Casanova J. Alzheimer's Disease Assessment Scale--cognitive in clinical practice. Int Psychogeriatr. 1997; 9(Suppl 1):105–114. [PubMed: 9447433]

Pihlajamaki M, Sperling RA. Functional MRI assessment of task-induced deactivation of the default mode network in Alzheimer's disease and at-risk older individuals. Behav Neurol. 2009; 21:77–91. [PubMed: 19847047]

Popa D, Popescu AT, Pare D. Contrasting Activity Profile of Two Distributed Cortical Networks as a Function of Attentional Demands. J Neurosci. 2009; 29:1191–1201. [PubMed: 19176827]

Putcha D, O'Keefe K, Laviolette P, O'Brien J, Greve D, Rentz DM, Locascio J, Atri A, Sperling R. Reliability of functional magnetic resonance imaging associative encoding memory paradigms in non-demented elderly adults. Hum Brain Mapp. 2011; 32:2027–2044. [PubMed: 21259385]

Rami L, Sala-Llonch R, Sole-Padulles C, Fortea J, Olives J, Llado A, Pena-Gomez C, Balasa M, Bosch B, Antonell A, Sanchez-Valle R, Bartres-Faz D, Molinuevo JL. Distinct functional activity of the precuneus and posterior cingulate cortex during encoding in the preclinical stage of Alzheimer's disease. J Alzheimers Dis. 2012a; 31:517–526. [PubMed: 22596271]

Rami L, Sole-Padulles C, Fortea J, Bosch B, Llado A, Antonell A, Olives J, Castellvi M, Bartres-Faz D, Sanchez-Valle R, Molinuevo JL. Applying the new research diagnostic criteria: MRI findings and neuropsychological correlations of prodromal AD. Int J Geriatr Psychiatry. 2012b; 27:127–134. [PubMed: 21384432]

Raz G, Jacob Y, Gonen T, Winetraub Y, Flash T, Soreq E, Hendler T. Cry for her or cry with her: context-dependent dissociation of two modes of cinematic empathy reflected in network cohesion dynamics. Soc Cogn Affect Neurosci. 2014; 9:30–38. [PubMed: 23615766]

Rissman J, Gazzaley A, D'Esposito M. Measuring functional connectivity during distinct stages of a cognitive task. Neuroimage. 2004; 23:752–763. [PubMed: 15488425]

Rytsar R, Fornari E, Frackowiak RS, Ghika JA, Knyazeva MG. Inhibition in early Alzheimer's disease: an fMRI-based study of effective connectivity. Neuroimage. 2011; 57:1131–1139. [PubMed: 21616155]

Sala-Llonch R, Pena-Gomez C, Arenaza-Urquijo EM, Vidal-Pineiro D, Bargallo N, Junque C, Bartres-Faz D. Brain connectivity during resting state and subsequent working memory task predicts behavioural performance. Cortex. 2012; 48:1187–1196. [PubMed: 21872853]

Scheff SW, Price DA. Synapse loss in the temporal lobe in Alzheimer's disease. Ann Neurol. 1993; 33:190–199. [PubMed: 8434881]

Schon K, Atri A, Hasselmo ME, Tricarico MD, LoPresti ML, Stern CE. Scopolamine reduces persistent activity related to long-term encoding in the parahippocampal gyrus during delayed matching in humans. J Neurosci. 2005; 25:9112–9123. [PubMed: 16207870]

Seeley WW, Crawford RK, Zhou J, Miller BL, Greicius MD. Neurodegenerative Diseases Target Large-Scale Human Brain Networks. Neuron. 2009; 62:42–52. [PubMed: 19376066]

Seeley WW, Menon V, Schatzberg AF, Keller J, Glover GH, Kenna H, Reiss AL, Greicius MD. Dissociable intrinsic connectivity networks for salience processing and executive control. J Neurosci. 2007; 27:2349–2356. [PubMed: 17329432]

Sepulcre J, Liu H, Talukdar T, Martincorena I, Yeo BTT, Buckner RL. The Organization of Local and Distant Functional Connectivity in the Human Brain. PLoS Computational Biology. 2010; 6:e1000808. [PubMed: 20548945]

Shehzad Z, Kelly C, Reiss PT, Cameron Craddock R, Emerson JW, McMahon K, Copland DA, Castellanos FX, Milham MP. A multivariate distance-based analytic framework for connectome-wide association studies. Neuroimage. 2014; 93(Pt 1):74–94. [PubMed: 24583255]

Simon JJ, Walther S, Fiebach CJ, Friederich HC, Stippich C, Weisbrod M, Kaiser S. Neural reward processing is modulated by approach- and avoidance-related personality traits. Neuroimage. 2010; 49:1868–1874. [PubMed: 19770056]

Smith SM, Fox PT, Miller KL, Glahn DC, Fox PM, Mackay CE, Filippini N, Watkins KE, Toro R, Laird AR, Beckmann CF. Correspondence of the brain's functional architecture during activation and rest. Proc Natl Acad Sci U S A. 2009; 106:13040–13045. [PubMed: 19620724]

Sperling R. Functional MRI studies of associative encoding in normal aging, mild cognitive impairment, and Alzheimer's disease. Ann N Y Acad Sci. 2007; 1097:146–155. [PubMed: 17413017]

Sperling R, Chua E, Cocchiarella A, Rand-Giovannetti E, Poldrack R, Schacter DL, Albert M. Putting names to faces: successful encoding of associative memories activates the anterior hippocampal formation. Neuroimage. 2003a; 20:1400–1410. [PubMed: 14568509]

Sperling R, Greve D, Dale A, Killiany R, Holmes J, Rosas HD, Cocchiarella A, Firth P, Rosen B, Lake S, Lange N, Routledge C, Albert M. Functional MRI detection of pharmacologically induced memory impairment. Proceedings of the National Academy of Sciences of the United States of America. 2002; 99:455–460. [PubMed: 11756667]

Sperling RA, Bates JF, Chua EF, Cocchiarella AJ, Rentz DM, Rosen BR, Schacter DL, Albert MS. fMRI studies of associative encoding in young and elderly controls and mild Alzheimer's disease. J Neurol Neurosurg Psychiatry. 2003b; 74:44–50. [PubMed: 12486265]

Sperling RA, Bates JF, Cocchiarella AJ, Schacter DL, Rosen BR, Albert MS. Encoding novel face-name associations: a functional MRI study. Hum Brain Mapp. 2001; 14:129–139. [PubMed: 11559958]

Sperling RA, LaViolette PS, O'Keefe K, O'Brien J, Rentz DM, Pihlajamäki M, Marshall G, Hyman BT, Selkoe DJ, Hedden T, Buckner RL, Becker JA, Johnson KA. Amyloid Deposition Is Associated with Impaired Default Network Function in Older Persons without Dementia. Neuron. 2009; 63:178–188. [PubMed: 19640477]

Van Essen DC. A Population-Average, Landmark- and Surface-based (PALS) atlas of human cerebral cortex. NeuroImage. 2005; 28:635–662. [PubMed: 16172003]

Vincent JL, Patel GH, Fox MD, Snyder AZ, Baker JT, Van Essen DC, Zempel JM, Snyder LH, Corbetta M, Raichle ME. Intrinsic functional architecture in the anaesthetized monkey brain. Nature. 2007; 447:83–86. [PubMed: 17476267]

Wang L, Zang Y, He Y, Liang M, Zhang X, Tian L, Wu T, Jiang T, Li K. Changes in hippocampal connectivity in the early stages of Alzheimer's disease: Evidence from resting state fMRI. Neuroimage. 2006; 31:496–504. [PubMed: 16473024]

Ward AM, Schultz AP, Huijbers W, Van Dijk KR, Hedden T, Sperling RA. The parahippocampal gyrus links the default-mode cortical network with the medial temporal lobe memory system. Hum Brain Mapp. 2013

Wig GS, Grafton ST, Demos KE, Wolford GL, Petersen SE, Kelley WM. Medial temporal lobe BOLD activity at rest predicts individual differences in memory ability in healthy young adults. Proc Natl Acad Sci U S A. 2008; 105:18555–18560. [PubMed: 19001272]

Research Highlights

1. Reveal robust correlations between task connectivity and cognitive performance
2. Reveal that there may be ‘coordinated’ brain states that underlie cognition
3. Observe connectivity changes within and between brain networks during task
4. Conclude that task connectivity is complementary to resting connectivity

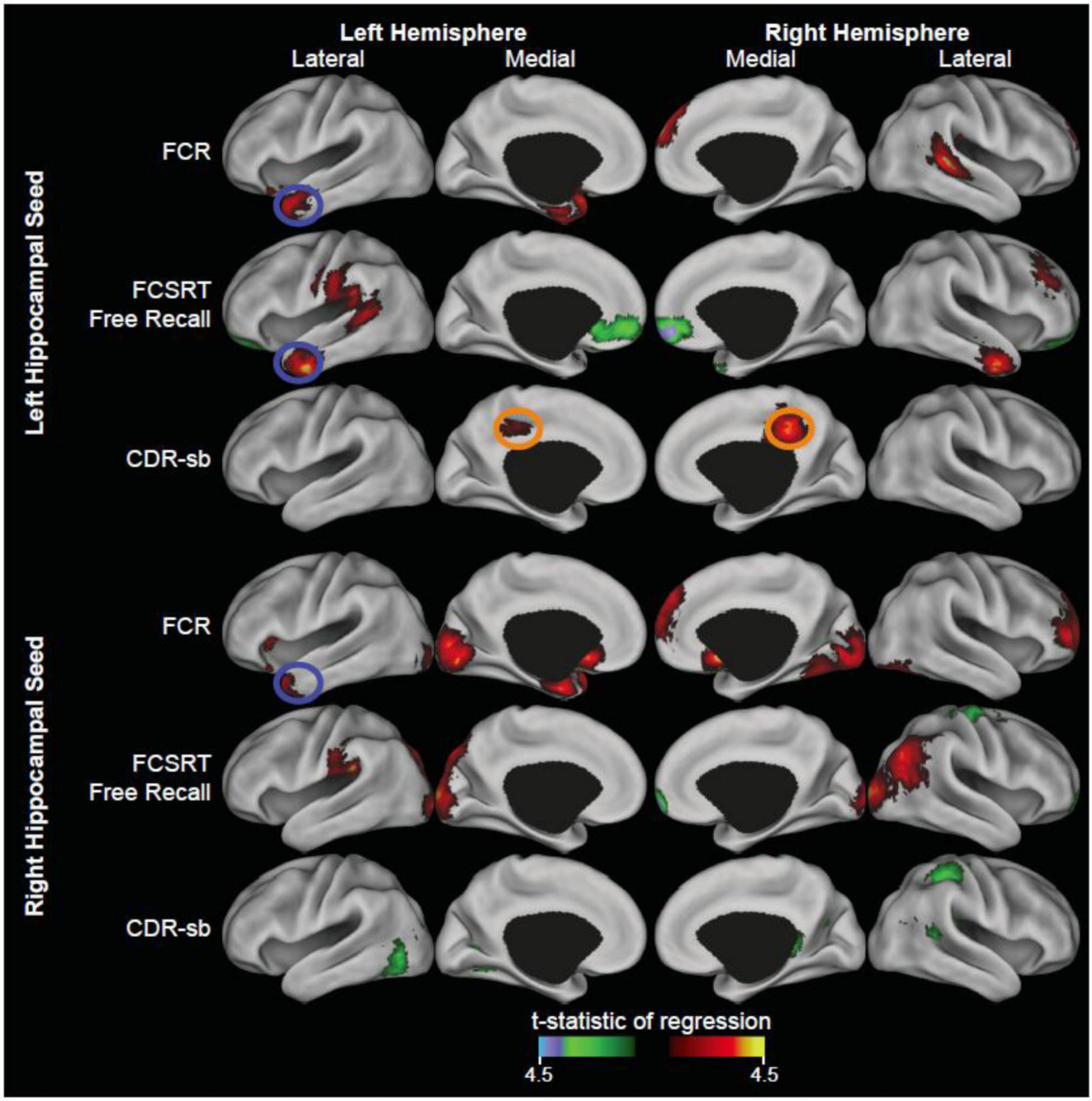

Figure 1. Exemplar PPI correlations with cognition

Cortical surface renderings on the PALS CARET surface (Van Essen, 2005) for ADAS-Cog Delayed Recall, CDR-sb, and FCSRT Free correlations with either the left hippocampal seed PPI (top rows) or the right hippocampal seed PPI (bottom rows) using multi-fiducial mapping with the strongest voxel within 2.5 mm of the surface. Results for each regression were thresholded at $p<0.01$ ($t=2.58$) and 174 contiguous voxels resulting in cluster corrected $p<0.05$. Red and yellow colors indicate regions where higher N>R PPI was associated with better performance. Green and blue colors indicate regions where where higher R>N PPI

was associated with better performance. Blue circles indicate common areas between the regressions of FCSRT Free-recall and ADAS-Cog Delayed Recall. Orange circles indicate common areas between the regressions of FCSRT Free and CDR-sb. Cyan circles indicate common areas between the regressions of ADAS-Cog Delayed Recall and CDR-sb.

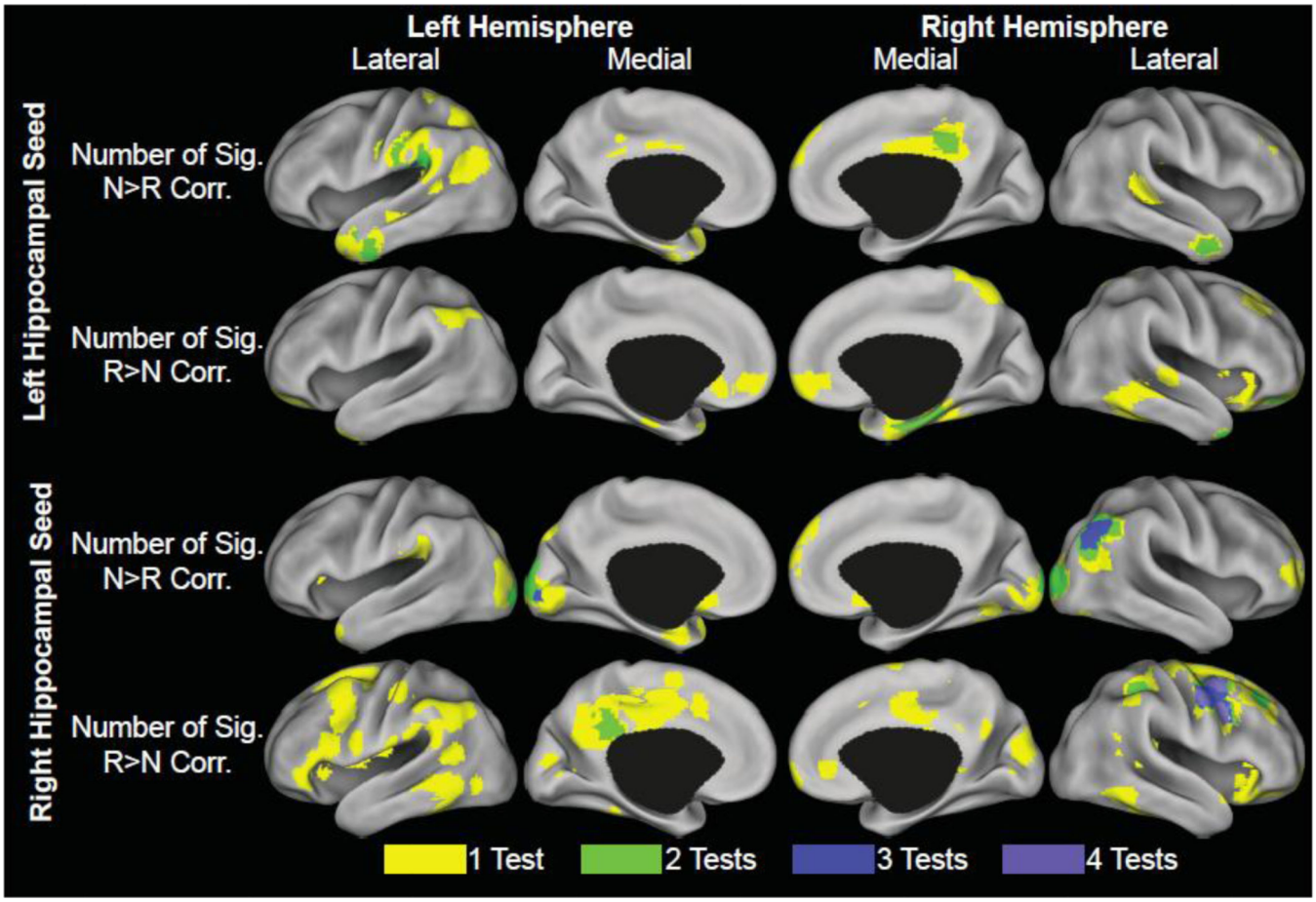

Figure 2. Overlap of PPI correlations with cognition

Cortical surface renderings on the PALS CARET surface (Van Essen, 2005) for the number of tests that reached significance at each voxel. The value of each node was based on the largest number of tests within 2.5 mm of PALS average fiducial surface. *Top row:* Number of tests at each location showing significant correlations between performance and the left hippocampal seed N>R PPI. *Second row:* Number of tests at each location showing significant correlations between performance and the left hippocampal seed R>N PPI. *Third row:* Number of tests at each location showing significant correlations between performance and the right hippocampal seed N>R PPI. *Bottom row:* Number of tests at each location showing significant correlations between performance and the right hippocampal seed R>N PPI. The maximum value was 5 tests; however, this did not fall within 2.5 mm of the average surface.

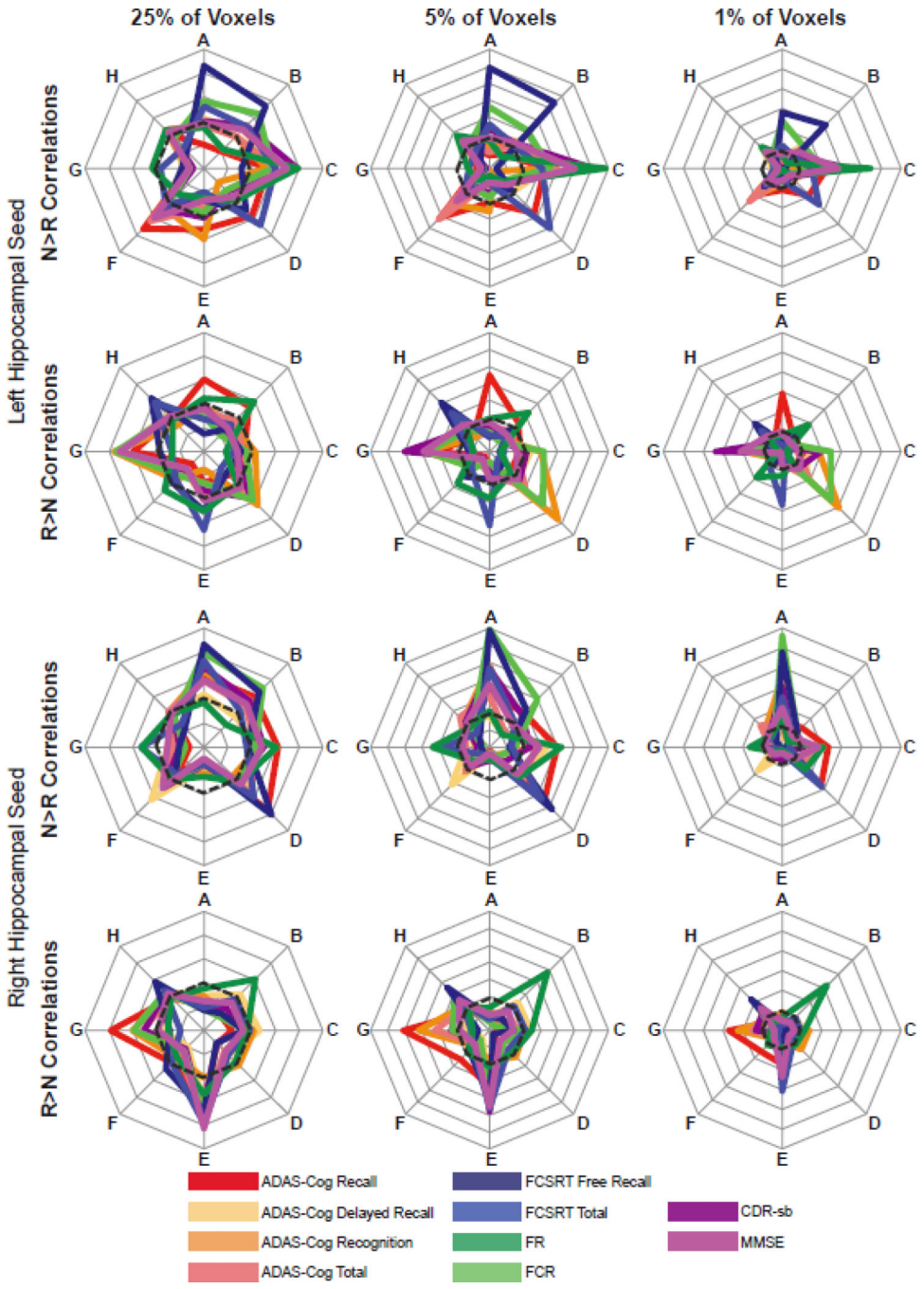

Figure 3. Spatial distribution of PPI correlations with cognition

Spatial distribution of PPI correlations by cortical network (Smith et al., 2009). From left to right, the plots are based on the top 25% of voxels showing correlations with the left hippocampal seed N>R PPI (top row) or correlations with the left hippocampal seed R>N PPI (second row) and the top 25% of voxels showing correlations with the right hippocampal seed N>R PPI (third row) or correlations with the right hippocampal seed R>N PPI (bottom row); the top 5% of voxels showing correlations with the left hippocampal seed N>R PPI (top row) or correlations with the left hippocampal seed R>N PPI (second row)

and the top 5% of voxels showing correlations with the right hippocampal seed N>R PPI (third row) or correlations with the right hippocampal seed R>N PPI (bottom row); the top 1% of voxels showing correlations with the left hippocampal seed N>R PPI (top row) or correlations with the left hippocampal seed R>N PPI (second row) and the top 1% of voxels showing correlations with the right hippocampal seed N>R PPI (third row) or correlations with the right hippocampal seed R>N PPI (bottom row);. For 25% of voxel plots, the outside ring is 0.5; for 5% of voxel plots, the outside ring is 0.15; and for 1% of voxel plots, the outside ring is 0.05. The dashed line are drawn at 0.25, 0.05, and 0.01 to indicate where the correlations would be expected if they were uniformly distributed across the networks, respectively. A: medial visual network; B: lateral visual network; C: default-mode network; D: cerebellum network; E: sensorimotor network; F: auditory network; G: executive control network; H: frontoparietal network.

Table 1

Demographics and Cognitive Tests

Demographics	
Age	71.63 (1.71)
Education	16.00 (0.57)
Gender (f/m)	9/15
Cognitive Tests	
FR (% correct)	67.00 (3.05)
FCR (% correct)	68.75 (3.31)
FCSRT-Free Recall (# correct)	10.08 (1.72)
FCSRT-Total (# correct)	30.54 (2.78)
ADAS-Cog Total (# of errors)	26.15 (1.90)
ADAS-Cog Recall (# of errors)	5.94 (0.35)
ADAS-Cog Delayed Recall (# of errors)	8.33 (0.39)
ADAS-Cog Recognition (# of errors)	6.71 (0.66)
MMSE (# correct)	24.04 (0.58)
CDR-SB (score)	4.67 (0.50)

For FCSRT, MMSE and post-scan Memory Tests higher scores indicate better performance. For CDR-SB and ADAS-Cog lower scores represent better performance. Values are the mean and standard error.

Table 2

Distribution of significant PPI results by anatomical region

AAL Region	ADAS Del. Recall L	ADAS Del. Recall R	ADAS Recall L	ADAS Recall R	ADAS Recog. L	ADAS Recog. R	ADAS Total L	ADAS Total R	FCSRT Free L	FCSRT Free R	FCSRT Total L	FCSRT Total R	FR L	FR R	FCR L	FCR R	CDR-SB L	CDR-SB R	MMSE L	MMSE R
Visual Network																				
L. Calcarine Sulcus						−										+++				
L. Cuneus						−−−			+	+						+++				
L. Lingual Gyrus		−−														+++				
L. Fusiform Gyrus	++				+++ −										+++	+				
L. Inf. Occipital Gyrus																+++				
L. Mid. Occipital Gyrus					+		+		+	+			−			+++			+	
L. Sup. Occipital Gyrus									+							+++	+			
L. Hippocampus		−−−											−		+++	+++				
Default-mode Network																				
L. Mid. Frontal Gyrus - Orb.									−−	−										
L. Olfactory Sulcus									−						++					
L. Inf. Temporal Gyrus	+++				+++ −−−				++	++			−−			+++				+
L. Mid. Temporal Gyrus	+++				+++ −−				+	++		+	−−−		++	+++	+			+++
L. Mid. Temporal Pole					−−−					+		+			+	++				+++
L. Parahippocampal Gyrus		−−−									−				+++	+++				
L. Angular Gyrus										++			−−−				+++			
L. Precuneus		−				−−−	++		++	++							+++	+++	+++	
L. Post. Cingulate Cortex	++					−−			+	+										
Sensorimotor Network																				
L. Paracentral Lobule									+	++				−						
L. Supp. Motor Area										−										
L. Precentral Gyrus													−							

AAL Region	ADAS Del. Recall L	ADAS Del. Recall R	ADAS Recall L	ADAS Recall R	ADAS Recog. L	ADAS Recog. R	ADAS Total L	ADAS Total R	FCSRT Free L	FCSRT Free R	FCSRT Total L	FCSRT Total R	FR L	FR R	FCR L	FCR R	CDR-SB L	CDR-SB R	MMSE L	MMSE R
L. Postcentral Gyrus	+++				+				++	++			−−							
Auditory Network																				
L. Amygdala															+++	+				
L. Heschl's Gyrus																				
L. Mid. Cingulate Cortex	++									+				−−−			+	++		
L. Insula					−				−				−		++	+				
L. Rolandic Operculum	+								+	+			−−−							
L. Sup. Temporal Gyrus	+								+	++		+				+	+++			
L. Sup. Temporal Pole					−					+		+			++	+++				+++
L. Inf. Frontal Gyrus - Orb.					−				−−											
Executive Control Network																				
L. Caudate						−		−−	−	−−			−	−						
L. Putamen									−	−					+					
L. Pallidum										−				−−						
L. Thalamus		−−−			−−−			−−−				−		−−						−−
L. Ant. Cingulate Cortex																				
L. Sup. Frontal Gyrus - Med.									−	−	−	−−								
Frontoparietal Network																				
L. Supramarginal Gyrus	+++								+	++							+++			
L. Inf. Parietal Lobule	++				+++		+			+			−−−				++		+	
L. Sup. Parietal Lobule					+++		+++		++	++							++	+	+++	
L. Inf. Frontal Operculum										−			−−							
L. Inf. Frontal Gyrus - pt										−										
L. Mid. Frontal Gyrus																				
L. Sup. Frontal Gyrus																				
L. Sup. Frontal Gyrus - Orb.									−−	−										
Visual Network																				

AAL Region	ADAS Del. Recall L	ADAS Del. Recall R	ADAS Recall L	ADAS Recall R	ADAS Recog. L	ADAS Recog. R	ADAS Total L	ADAS Total R	FCSRT Free L	FCSRT Free R	FCSRT Total L	FCSRT Total R	FR L	FR R	FCR L	FCR R	CDR-SB L	CDR-SB R	MMSE L	MMSE R
R. Calcarine Sulcus										++						++				
R. Cuneus										+						+++				
R. Lingual Gyrus		−−−	−−		−			−−				−				++				−−−
R. Fusiform Gyrus					−−	−			+	+	−		−−−			++				
R. Inf. Occipital Gyrus																++				
R. Mid. Occipital Gyrus						+	+	+		++				−−		+++				
R. Sup. Occipital Gyrus										++						+++				
R. Hippocampus					−−				+							+++				
Default-mode Network																				
R. Mid. Frontal Gyrus - Orb.					−−−	−−			−	−−		−								
R. Olfactory Sulcus									−											
R. Inf. Temporal Gyrus	+++								++	++			−−−			++				
R. Mid. Temporal Gyrus	+++			+					++	++			−−−	−−−	++	++				
R. Mid. Temporal Pole	+++				−−−				++	+	−−−									
R. Parahippocampal Gyrus					−−−	−					−									
R. Angular Gyrus			++	+++		++	+++	+++		++				−−		+				
R. Precuneus		−−−	−					−−		+		−	−−−			++	++	+		−−−
R. Post. Cingulate Cortex	++							−				−					++			−−
Sensorimotor Network																				
R. Paracentral Lobule																				
R. Supp. Motor Area										−−			−−	−−						
R. Precentral Gyrus									++	−		−	−−−							−
R. Postcentral Gyrus									++				−−−							
Auditory Network																				
R. Amygdala					−−															
R. Heschl's Gyrus						++						+			+					
R. Mid. Cingulate Cortex	++											−−		−−			+++			

AAL Region	ADAS Del. Recall L	ADAS Del. Recall R	ADAS Recall L	ADAS Recall R	ADAS Recog. L	ADAS Recog. R	ADAS Total L	ADAS Total R	FCSRT Free L	FCSRT Free R	FCSRT Total L	FCSRT Total R	FR L	FR R	FCR L	FCR R	CDR-SB L	CDR-SB R	MMSE L	MMSE R
R. Insula					−−	+++ −−−					−	+ −		−						
R. Rolandic Operculum						+++						+			+++	++				
R. Sup. Temporal Gyrus				+		+	+	++	+	++		+	−−−		+++	+++				
R. Sup. Temporal Pole					−−						−	+								
R. Inf. Frontal Gyrus - Orb.					−−−	−−−			−	−		−								
Executive Control Network																				
R. Caudate						−		−−	−	−			−	−						
R. Putamen						−−				−			−−−	−−−						
R. Pallidum										−			−−	−−						
R. Thalamus		−−−			−−−			−−					−	−−−						−
R. Ant. Cingulate Cortex									−	−										
R. Sup. Frontal Gyrus - Med.									−−	−−				−−	+++					
Frontoparietal Network																				
R. Supramarginal Gyrus						+	+	+						−−−		+++				
R. Inf. Parietal Lobule			++	+		+								−−−						
R. Sup. Parietal Lobule													−−−	−−						
R. Inf. Frontal Operculum						++						+	−							−
R. Inf. Frontal Gyrus - pt						−			+	−		−					++			−
R. Mid. Frontal Gyrus								−	++	−	+++	−	−−−	−−−	++		+++		+++	−−−
R. Sup. Frontal Gyrus								−	−	−		−	−−	−−−	+++				++	−−
R. Sup. Frontal Gyrus - Orb					−−−	−			−−	−−		−								

Columns are the left and right hippocampal seed regions. Regions are divided into functional networks based on the resting state maps from Smith and colleagues (2009). L., left; R., right; Ant., anterior; Inf., inferior; Sup., superior; Mid, middle; Orb., orbital part; pt, pars triangularis; Med., medial; and Supp., supplementary. +,++,+++ and −,−−,−−− indicate the lower, middle, and upper tertiles of t-statistics for N>R and R>N, respectively. Regions highlighted in yellow represent key areas that hold potential as functional biomarkers.